



Structural properties and in vitro evaluation of some Ln (III) complexes as potential selective antimicrobial and antioxidant substances

Ahmed K. Hijazi¹ · Ziyad A. Taha¹ · Abdellatif Ibdah¹ · Idris M. Idris¹ · Waleed M. Al-Momani²

Received: 27 January 2021 / Accepted: 22 April 2021
© Institute of Chemistry, Slovak Academy of Sciences 2021

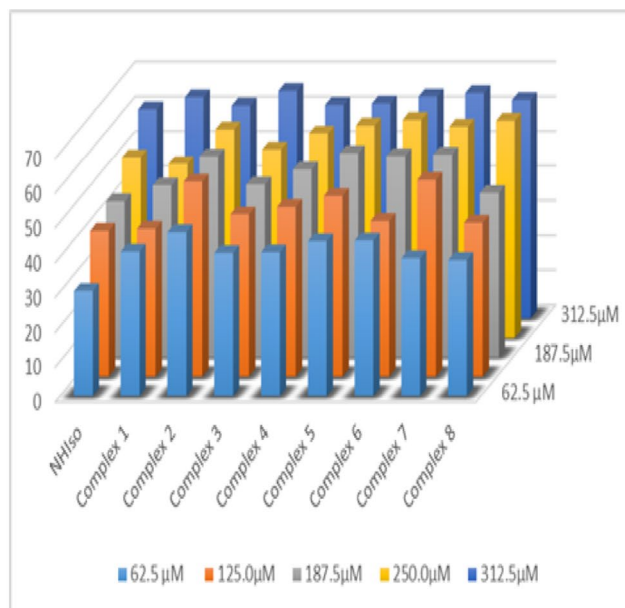
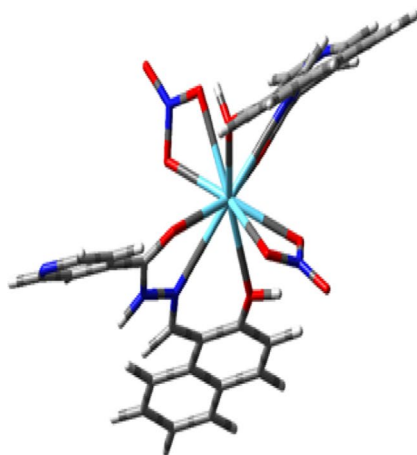
Abstract

Rare metals have been used in pharmaceuticals and for medicinal purposes for long time. Currently, the link between some specific medicinal and biological properties of inorganic drugs has been established. $[\text{Ln}(\text{NO}_3)_3]$ complexes with *N*-(2-hydroxynaphthalen-1-yl) methylene) isonicotinohydrazide Schiff base, $[\text{Ln}(\text{NHiso})_2(\text{NO}_3)_2]\text{NO}_3$, complexes **1–8**, were prepared and characterized using different techniques. The expected coordination for prepared complexes is ten, six from the tri-dentate NHiso ligand, and four from the two bi-dentate nitrate groups. DFT calculations on La and its cationic $[\text{La}(\text{NHiso})_2(\text{NO}_3)_2]^+$ complex were carried out at the B3LYP level of theory. The NHiso ligand and its lanthanide complexes were screened for antimicrobial activity, in vitro activity against four gram-negative bacteria *Ec: Escherichia coli*; *Kp: Klebsiella pneumonia*; *Pm: Proteus mirabilis*; *Pa: Pseudomonas aeruginosa*, with two gram-positive bacteria *En: Enterococcus faecalis* and *Sa: Staphylococcus aureus*. Complexes **1, 2, 4, 7** and **8** showed excellent and higher activity against *En* and *Sa* Gram-positive bacteria than the free ligand, especially complex **2** with a MIC value of 4 $\mu\text{g}/\text{mL}$. The reported complexes have greater and significant efficiency in quenching DPPH than that of free NHiso ligand, with a scavenging activity between 39 and 65%.

Extended author information available on the last page of the article

Graphic Abstract

Ln(III) nitrate complexes with *N*-(2-hydroxynaphthalen-1-yl) methylene) isonicotinohydrazide Schiff base, $[\text{Ln}(\text{NHiso})_2(\text{NO}_3)_2]\text{NO}_3$, were prepared and characterized. They showed very promising antimicrobial and antioxidant activities. Their molecular geometries have been examined using DFT calculations and the obtained results are in good agreement with the experimental data.



Keywords Hydrazone Schiff base · Lanthanides complexes · DFT · MIC · Antibacterial · Antioxidant

Introduction

Lanthanides complexes have a diversity of applications in bioinorganic chemistry, catalysis, luminescence and medicinal chemistry (Bünzli 2008; Al Momani et al. 2013; Chandrasekhar et al. 2013; Ghozlan et al. 2011; Taha and Hijazi 2021). Literature studies show that Ln(III) complexes have higher antibacterial and antioxidant activities than their corresponding Schiff base ligands (Kumar et al. 2009; Hijazi et al. 2017a, b; Taha et al. 2018; Ameen et al. 2018; Jin et al. 2017). Ameen et al. revealed that their synthesized Pr(III) complexes can act as good antibacterial and mild antifungal substances. Hijazi et al. showed that their lanthanide complexes derived from *N*-(2-hydroxynaphthalen-1-yl) methylene) nicotinohydrazide Schiff base have moderate activities against different strains of bacteria.

These type of complexes have luminescent properties which make them useful substances in a variety of applications, such as: liquid crystals, light emission diodes, biophysics and optical systems (Gao et al. 2018; Wang et al. 2019; Singh et al. 2007; Cai et al. 2021; Andres and Chauvin 2020). Luminescent Ln(III) ions have unique emission bands

due to $f-f$ transitions. These trivalent ions are capable of producing luminescence by photosensitization when coordinated with organic ligands bearing a chromophore with appropriate photophysical properties.

Metal complexes containing hydrazones as Schiff bases have been studied in details due to their antimicrobial and industrial uses (Canpolat and Kaya 2004; Palai et al. 2018; Desoky et al. 2019). The studies show, that in all cases, the metal complexes screened against different types of bacteria (Gram-positive and Gram-negative) and against fungi, act as more potent agents than their hydrazine ligands. P, S, N and O presence as donor atoms in many Schiff bases, gave them an importance in biology by inhibiting the growth of bacteria (Xu et al. 2010). The ones which contain (C=N) gives delocalization associated with extended conjugation by forming an extreme chelated ring (Abdel-Rahman et al. 2017a, b; Belicchi et al. 2001; Abu-Dief et al. 2020).

Biologically active species bonded to metal ions have enhanced the activities of the synthesized complexes. Many research groups showed the synthesis of a variety of Ln(III) complexes containing mono-, bi- and tri-dentate hydrazones, which have interesting biological and therapeutic activities

(Khan and Sharma 2008; Agarwala et al. 1990). Acylhydrazones belong to Schiff base family with keto-type structure ($-\text{O}=\text{C}-\text{N}=\text{N}=\text{C}-$) contain π -bonds and a variety of heteroatoms. These types of complexes have been studied due to their biological activity. They have been reported to possess, antimalarial, antitubercular, analgesic, anti-inflammatory, antibacterial, antifungal, antiviral, antiplatelet, antioxidant and antitumoral activities (Taha et al. 2015; Avaji et al. 2009; Aziz et al. 2014; Bayrak et al. 2009). Of the most widely used drugs for the treatment of tuberculosis, are the ones that contain isonicotinic acid hydrazide and pyrazinamide (Gudasi et al. 2007; Gulerman et al. 2000).

A wide range of hydrazones and their derived compounds have been reported for their antibacterial activities against different types of bacteria (Kuriakose et al. 2007; Hijazi et al. 2017a).

It is hypothesized that there is a strong link and correlation between Schiff bases and complexes derived from them, containing transition metals and lanthanides, as inorganic drugs, and their medicinal and biological properties (antibacterial and antioxidant). In this paper, the preparation, characterization, luminescence, density functional theory (DFT) and biological studies and activities of eight novel Ln(III) nitrate complexes with isonicotinohydrazide Schiff base is reported. The antioxidant, antibacterial, luminescence and DFT properties have been studied. This present work is considered a continuation study, of our research group, on the lanthanides and transition metals chemistry (Taha et al. 2017a, b; Ajlouni et al. 2018, 2019; Taha et al. 2018, 2020; Hijazi et al. 2020, 2021; Taha et al. 2017a, b).

Experimental

The NHiso ligand was prepared according to literature (Khan and Sharma 2008). Analytical grade solvents, $[\text{Sm}(\text{NO}_3)_3 \cdot 6\text{H}_2\text{O}]$, $[\text{La}(\text{NO}_3)_3 \cdot 6\text{H}_2\text{O}]$, $[\text{Nd}(\text{NO}_3)_3 \cdot 6\text{H}_2\text{O}]$, $[\text{Pr}(\text{NO}_3)_3 \cdot 6\text{H}_2\text{O}]$, $[\text{Er}(\text{NO}_3)_3]$, $[\text{Gd}(\text{NO}_3)_3 \cdot 6\text{H}_2\text{O}]$, $[\text{Dy}(\text{NO}_3)_3 \cdot \text{H}_2\text{O}]$, $[\text{Eu}(\text{NO}_3)_3 \cdot 5\text{H}_2\text{O}]$, 2-hydroxy-1-naphthaldehyde and isonicotinic hydrazide, were purchased from Merck (Germany) and used as received. Flash 2000 elemental analyzer (Thermo Fischer Scientific, Germany) was used to perform elemental analyses of C, H and N. The complexes lanthanides content was determined by titration with Ethylenediaminetetraacetic acid disodium salt (EDTA) using an indicator (xylenol orange) and a buffer (acetic acid) purchased from Merck (Germany). Bruker ALPHA spectrophotometer (Bruker, Germany) was used to record FT-IR spectra in the region of $4000\text{--}400\text{ cm}^{-1}$. Bruker Avance 400 MHz and 100 MHz spectrometer (Bruker Corporation, United States) was used to record the ^1H and ^{13}C NMR

spectra, respectively. Tetramethylsilane (TMS) was used as an internal standard for measuring the chemical shifts in deuterated dimethylsulphoxide ($\text{DMSO-}d_6$). Molar conductivities were measured at 298 K, 10^{-4} M concentration, in DMSO solution, using WTW LF 318 conductivity meter (Jenway Company, United Kingdom). UV-Visible spectra were recorded at 298 K, 10^{-6} M concentration, in DMSO solution, using a UV-2550 spectrophotometer (Schimadzu Corporation, Japan). Edinburgh FS900SDT spectrometer was used to record luminescent spectra in DMSO solution with 1.0 cm quartz cell. Scanning of the emission is carried out at wavelength that varied from 200 to 700 nm. Thermal analysis was performed on a PCT-2A thermo-balance analyzer (B.R.A.H.M.S GmbH, Germany) in the range of $20\text{--}900\text{ }^\circ\text{C}$ operating at a heating rate of $10\text{ }^\circ\text{C}/\text{min}$ under N_2 . Scanning electron microscope images (SEM) were performed using Quanta FEG 450 microscope equipped with Everhart Thornley Detector (FEI company, United States).

Preparation of complexes

The Ln(III) complexes were synthesized according the following procedure: 30 mL acetonitrile solution of 0.2 g (0.68 mmol) of NHiso, was charged to 30 mL ethyl ethanoate solution of 0.34 mmol of $\text{Ln}(\text{NO}_3)_3 \cdot x\text{H}_2\text{O}$ salts. The overall solution was stirred for 120 min., at room temperature. Filtration was used to separate the formed precipitate. It was washed many times with acetonitrile and ethyl ethanoate (50:50) solution mixture using a Buchner funnel with a sintered glass disk for purification. The precipitate was dried, under normal atmosphere at room temperature, for 24 h.

$[\text{La}(\text{NHiso})_2(\text{NO}_3)_2]\text{NO}_3$ complex 1

For $\text{C}_{44}\text{H}_{56}\text{LaN}_9\text{O}_{13}$ (1057.87), Calcd. (%): C, 45.00; H, 2.89; N, 13.89; La, 15.31. Found (%): C, 44.89; H, 2.95; N, 13.76; La, 15.26. $\Lambda_m = 88.7\ \Omega^{-1}\text{ cm}^{-1}\text{ mol}^{-1}$. Selected IR (KBr, cm^{-1}): $\nu(\text{OH})$ 3433, $\nu(\text{C}=\text{N})$ 1613, $\nu(\text{NO}_3^-)$ 1384, $\nu(\text{M}-\text{N})$ 432, $\nu(\text{M}-\text{O})$ 411. $^1\text{H-NMR}$: δ (OH) 12.55 ppm, (CH=N) 8.84 ppm, (C=N) 9.47 ppm. $^{13}\text{C-NMR}$: δ (C=O) 160.94 ppm, (C=N) 139.75 ppm. Yield: 85%.

$[\text{Pr}(\text{NHiso})_2(\text{NO}_3)_2]\text{NO}_3$ complex 2

For $\text{C}_{44}\text{H}_{56}\text{PrN}_9\text{O}_{13}$ (1059.87), Calcd. (%): C, 44.90; H, 2.88; N, 13.86; La, 15.49. Found (%): C, 44.72; H, 2.96; N, 13.94; La, 15.50. $\Lambda_m = 113.2\ \Omega^{-1}\text{ cm}^{-1}\text{ mol}^{-1}$. Selected IR (KBr, cm^{-1}): $\nu(\text{OH})$ 3432, $\nu(\text{C}=\text{N})$ 1613, $\nu(\text{NO}_3^-)$ 1384, $\nu(\text{M}-\text{N})$ 431, $\nu(\text{M}-\text{O})$ 412. Yield: 86%.

[Nd(NHiso)₂(NO₃)₂]NO₃ complex 3

For C₄₄H₅₆NdN₉O₁₃ (1063.20), Calcd. (%): C, 44.73; H, 2.87; N, 13.81; La, 15.80. Found (%): C, 44.80; H, 2.85; N, 13.70; La, 15.87. $\Lambda_m = 113.7 \Omega^{-1} \text{ cm}^{-1} \text{ mol}^{-1}$. Selected IR (KBr, cm⁻¹): $\nu(\text{OH})$ 3432, $\nu(\text{C}=\text{N})$ 1614, $\nu(\text{NO}_3^-)$ 1384, $\nu(\text{M}-\text{N})$ 432, $\nu(\text{M}-\text{O})$ 411. Yield: 73%.

[Sm(NHiso)₂(NO₃)₂]NO₃ complex 4

For C₄₄H₅₆SmN₉O₁₃ (1069.32), Calcd. (%): C, 44.44; H, 2.85; N, 13.81; La, 16.36. Found (%): C, 44.57; H, 2.86; N, 13.66; La, 16.50. $\Lambda_m = 90.5 \Omega^{-1} \text{ cm}^{-1} \text{ mol}^{-1}$. Selected IR (KBr, cm⁻¹): $\nu(\text{OH})$ 3432, $\nu(\text{C}=\text{N})$ 1613, $\nu(\text{NO}_3^-)$ 1384, $\nu(\text{M}-\text{N})$ 432, $\nu(\text{M}-\text{O})$ 413. Yield: 70%.

[Eu(NHiso)₂(NO₃)₂]NO₃ complex 5

For C₄₄H₅₆EuN₉O₁₃ (1070.92), Calcd. (%): C, 44.36; H, 2.85; N, 13.69; La, 16.51. Found (%): C, 44.24; H, 2.76; N, 13.73; La, 16.36. $\Lambda_m = 111.9 \Omega^{-1} \text{ cm}^{-1} \text{ mol}^{-1}$. Selected IR (KBr, cm⁻¹): $\nu(\text{OH})$ 3432, $\nu(\text{C}=\text{N})$ 1614, $\nu(\text{NO}_3^-)$ 1383, $\nu(\text{M}-\text{N})$ 431, $\nu(\text{M}-\text{O})$ 412. Yield: 71%.

[Gd(NHiso)₂(NO₃)₂]NO₃ complex 6

For C₄₄H₅₆GdN₉O₁₃ (1076.21), Calcd. (%): C, 44.11; H, 2.83; N, 13.62; La, 16.98. Found (%): C, 44.24; H, 2.78; N, 13.79; La, 17.04. $\Lambda_m = 95.0 \Omega^{-1} \text{ cm}^{-1} \text{ mol}^{-1}$. Selected IR (KBr, cm⁻¹): $\nu(\text{OH})$ 3433, $\nu(\text{C}=\text{N})$ 1612, $\nu(\text{NO}_3^-)$ 1383, $\nu(\text{M}-\text{N})$ 432, $\nu(\text{M}-\text{O})$ 411. Yield: 73%.

[Dy(NHiso)₂(NO₃)₂]NO₃ complex 7

For C₄₄H₅₆DyN₉O₁₃ (1081.46), Calcd. (%): C, 43.85; H, 2.81; N, 13.54; La, 17.45. Found (%): C, 43.69; H, 2.89; N, 13.43; La, 17.46. $\Lambda_m = 111.7 \Omega^{-1} \text{ cm}^{-1} \text{ mol}^{-1}$. Selected IR (KBr, cm⁻¹): $\nu(\text{OH})$ 3433, $\nu(\text{C}=\text{N})$ 1614, $\nu(\text{NO}_3^-)$ 1384, $\nu(\text{M}-\text{N})$ 432, $\nu(\text{M}-\text{O})$ 411. Yield: 73%.

[Er(NHiso)₂(NO₃)₂]NO₃ complex 8

For C₄₄H₅₆ErN₉O₁₃ (1086.22), Calcd. (%): C, 43.63; H, 2.80; N, 13.47; La, 17.87. Found (%): C, 43.72; H, 2.74; N, 13.87; La, 17.76. $\Lambda_m = 113.3 \Omega^{-1} \text{ cm}^{-1} \text{ mol}^{-1}$. Selected IR (KBr, cm⁻¹): $\nu(\text{OH})$ 3423, $\nu(\text{C}=\text{N})$ 1612, $\nu(\text{NO}_3^-)$ 1384, $\nu(\text{M}-\text{N})$ 431, $\nu(\text{M}-\text{O})$ 412. Yield: 80%.

Antibacterial activities

The antibacterial activities of NHiso and the prepared complexes, **1–8**, were measured using micro-broth dilution minimum inhibition concentration against different strains

of bacteria [Gram-negative bacteria: *Escherichia coli* (*Ec*); *Klebsiella pneumonia* (*Kp*); *Proteus mirabilis* (*Pm*); *Pseudomonas aeruginosa* (*Pa*); Gram-positive bacteria: *Enterococcus faecalis* (*En*); *Staphylococcus aureus* (*Sa*)] (Hijazi et al. 2017a). A stock solution of DMSO of each antibacterial was prepared according to NCCLS guidelines. The MIC was done in standard sterile 96 well flat bottom plates and the layout was designed so that each row covered the antibacterial dilution of 16–0.015 µg/mL with one control well with no chemical. Using sterilized pipette, a 40 µL of each antibacterial with the wanted concentration was added to each well and another well was filled with the same control volume [DMSO (–ve control) and Oxytetracycline (+ve control)]. About 150 µL of Mueller Hinton medium was added to all wells, followed by a 10 µL of the bacterial culture. After sealing the plates, incubation at 310 K under normal conditions was done. After 24 h incubation, Eliza reader was used to read the microtitre plates.

Antioxidant activities

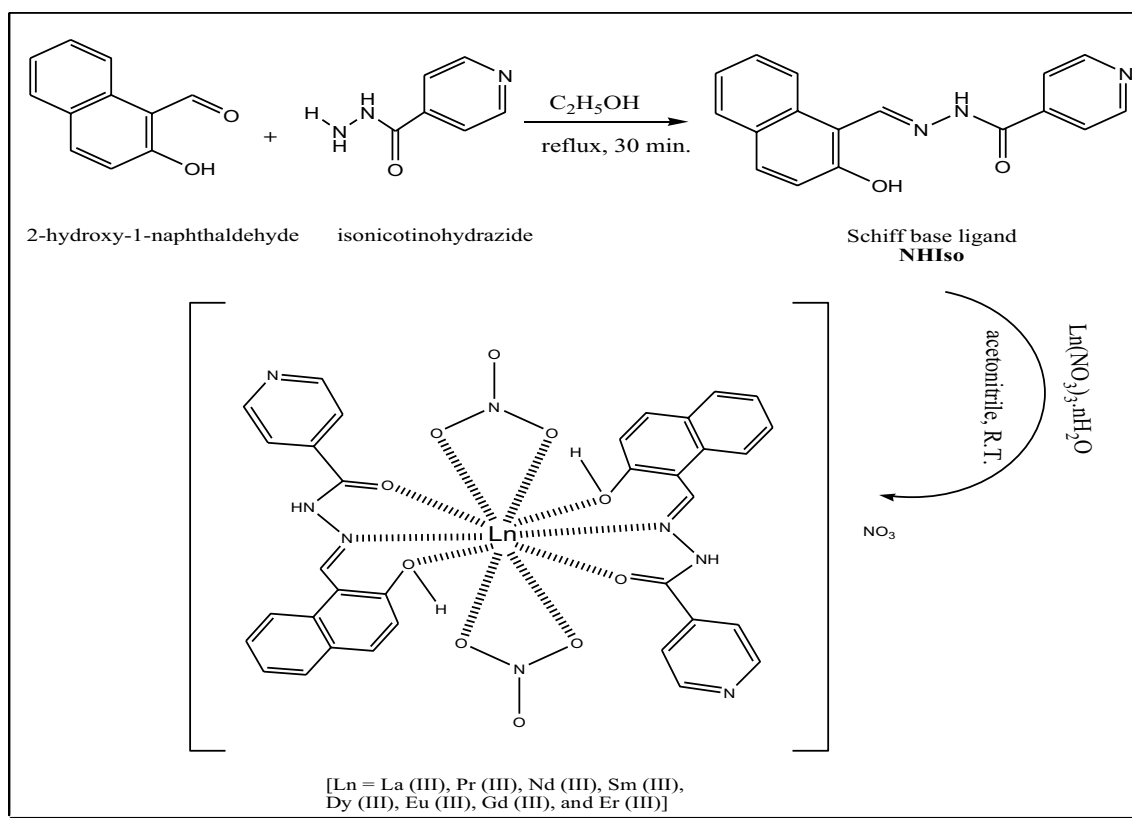
The antioxidant activities of NHiso and its prepared complexes, **1–8**, were measured and tested according to literature (Hijazi et al. 2017a), using a UV-2401PC UV–Visible spectrophotometer. 5×10^{-4} M solutions of all tested samples and Diphenyl-1-picrylhydrazyl (DPPH) were prepared in DMSO. A 500, 1000, 1500, 2000 and 2500 µL of each tested compound and 400 µL of DPPH solution was added to fill up volume of 4 mL to get final concentration of 62.5, 125, 187.5, 250 and 312.5 µM of tested compound and 50 µM of the DPPH as a control, 400 µL from DPPH solution was diluted using DMSO to 4.0 mL.

Computational method

Computations were carried out using the DFT (B3LYP) calculation in GAUSSIAN 03 program using the 6-31G(d) basis set for all atoms except for La LANL2TZ effective core potential basis set with *f* polarization functions has been used. The structure was verified to be minimum through calculating hessian vibrational frequencies at the same level of theory and basis sets that are used for optimization.

Results and discussion

In this work, the NHiso ligand was synthesized by conventional one step reaction of 2-hydroxy-1-naphthaldehyde with Isonicotinic Hydrazide in a 1:1 molar ratio following same procedure as described in the literature (Khan and Sharma 2008). The ligand was characterized using different spectroscopic techniques. The NHiso ligand was found to be soluble in DMSO and DMF.



Scheme 1 Synthesis of NHiso ligand and its Ln(III) complexes

Table 1 FT-IR values of the NHiso ligand and complexes **1–8**

Complex	$\nu(\text{OH})$	$\nu(\text{N-H})$	$\nu(\text{C=O})$	$\nu(\text{C=N})$	$\nu(\text{NO}_3^-)$						$\nu(\text{M-N})$	$\nu(\text{M-O})$
					ν_1	ν_2	ν_3	ν_4	$\nu_1-\nu_4$	ν_0		
NHiso	3440	3222	1692	1620	–	–	–	–	–	–	–	–
Complex 1	3433	3222	–	1614	1463	1031	815	1284	179	1384	433	411
Complex 2	3432	3221	–	1613	1464	1032	816	1284	180	1384	432	412
Complex 3	3432	3220	–	1613	1464	1032	815	1285	179	1382	433	411
Complex 4	3432	3222	–	1614	1463	1031	815	1284	178	1384	433	413
Complex 5	3432	3221	–	1614	1463	1033	815	1285	179	1383	432	412
Complex 6	3433	3222	–	1612	1464	1032	817	1285	178	1383	433	411
Complex 7	3432	3222	–	1614	1463	1032	816	1284	179	1384	433	411
Complex 8	3423	3222	–	1612	1462	1032	815	1285	177	1384	435	412

Complexes **1–8** were synthesized by reacting the NHiso ligand with lanthanide nitrate hydrate ($\text{Ln}(\text{NO}_3)_3 \cdot n\text{H}_2\text{O}$, where Ln: La(III), Sm(III), Gd(III), Pr(III), Nd(III), Er(III), Dy(III) and Eu(III), in 2:1 mol ratio, in an acetonitrile-ethyl ethanoate solution at room temperature. A group of complexes that correspond to the molecular formula of $[\text{Ln}(\text{NHiso})_2(\text{NO}_3)_2]\text{NO}_3$, complexes **1–8**, were obtained, Scheme 1. All prepared complexes, **1–8**, are soluble in DMSO and DMF, non-hygroscopic and stable in normal laboratory atmosphere.

Molar Conductance

Molar conductivities of NHiso ligand and all complexes are listed in the experimental part. The molar conductivity values for complexes **1–8** in DMSO solution are in the range $88.7\text{--}113.7 \Omega^{-1} \text{cm}^{-1} \text{mol}^{-1}$ at room temperature. They are in accordance with reported for 1:1 electrolyte (Geary 1971). Molar conductivity data suggest that two nitrates are coordinated directly to the Ln metal ions through the inner sphere, while the third exist at the outer coordination sphere.

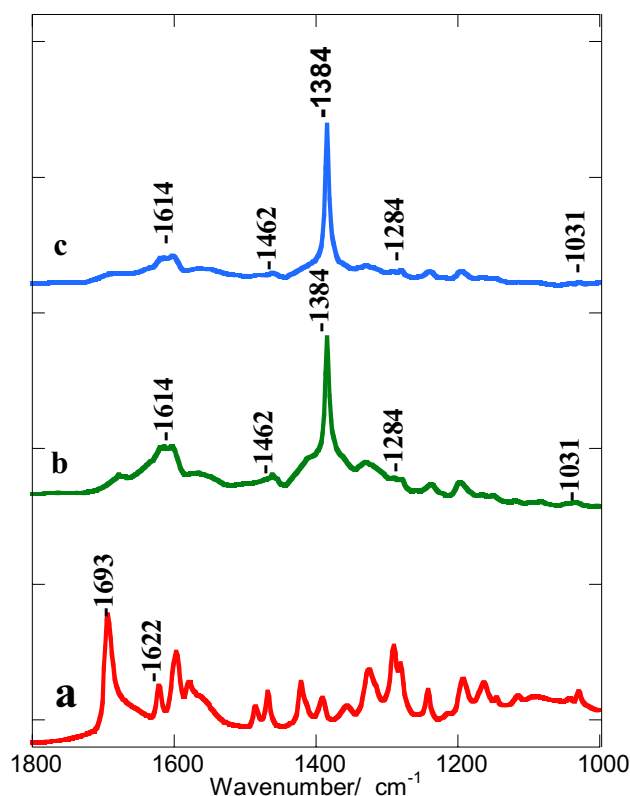


Fig. 1 FT-IR spectra of (a) NHiso; (b) complex 1; (c) complex 4

Fourier transform infrared (FT-IR) spectroscopy

Table 1 summarizes the important FT-IR spectral data of the NHiso ligand and complexes 1–8. The characteristic bands of the Schiff base ligand along with the expected shifts due to complexation with the Ln(III) ions are displayed in the spectra. The IR spectrum of NHiso shows the stretching vibration of (C=N) group at 1620 cm^{-1} , while showing a strong C=O stretching band at 1692 cm^{-1} , Fig. 1. Upon complexation, the C=O band disappeared in the spectra of all complexes 1–8, strongly suggesting enolization process is taking place during complexation (Biradar and Kulkarni 1971). The spectrum of the free NHiso shows a vibration band at 3440 cm^{-1} which is attributed to the –OH group, which shifts slightly, after complex formation, to 3432 cm^{-1} . The band of the –NH group of the free ligand is observed at 3222 cm^{-1} , still un-shifted after complexation. This may be attributed to the coordination through –OH, C=O and C=N groups.

The IR spectra of complexes 1–8 indicate that a coordination bond and chelation occur through the C=N group of the ligand due to the shift in the wavenumber of this group to a lower one as seen clearly in Table 1, (Abdel-Rahman et al. 2016a, b, 2017a; Sengupta et al. 1998; Donia and El-Boraey 2002). In the range $432\text{--}435\text{ cm}^{-1}$ and $411\text{--}413\text{ cm}^{-1}$ new

Table 2 Spectral data of NHiso and complexes 1–8

Complex	λ_{max} (nm)	Absorbance	Band Assignments
NHiso	326	0.091	$\pi \rightarrow \pi^*$
	328	0.091	$\pi \rightarrow \pi^*$
	349	0.092	$\pi \rightarrow \pi^*$
	416	0.122	$n \rightarrow \pi^*$
Complex 1	314	0.057	$\pi \rightarrow \pi^*$
	328	0.081	$\pi \rightarrow \pi^*$
Complex 2	369	0.098	$n \rightarrow \pi^*$
	313	0.229	$\pi \rightarrow \pi^*$
Complex 3	328	0.241	$\pi \rightarrow \pi^*$
	368	0.251	$n \rightarrow \pi^*$
	315	0.195	$\pi \rightarrow \pi^*$
Complex 4	328	0.230	$\pi \rightarrow \pi^*$
	368	0.241	$n \rightarrow \pi^*$
	314	0.189	$\pi \rightarrow \pi^*$
Complex 5	328	0.221	$\pi \rightarrow \pi^*$
	368	0.227	$n \rightarrow \pi^*$
	316	0.165	$\pi \rightarrow \pi^*$
Complex 6	328	0.221	$\pi \rightarrow \pi^*$
	368	0.249	$n \rightarrow \pi^*$
	313	0.233	$\pi \rightarrow \pi^*$
Complex 7	328	0.248	$\pi \rightarrow \pi^*$
	369	0.256	$n \rightarrow \pi^*$
	314	0.136	$\pi \rightarrow \pi^*$
Complex 8	328	0.155	$\pi \rightarrow \pi^*$
	368	0.155	$n \rightarrow \pi^*$
	314	0.158	$\pi \rightarrow \pi^*$
	328	0.204	$\pi \rightarrow \pi^*$
	368	0.214	$n \rightarrow \pi^*$

bands, with different intensities, were observed in the spectra of complexes 1–8, that were not present in the spectrum of the NHiso. These new bands are characteristic for the stretching vibration of M–N and M–O, respectively (Pandey et al. 1987).

Coordination of the nitrate ligand to the metal ion may occur in three types, mono-dentate and bi-dentate ligand within the inner coordination sphere, or as uncoordinated ion in the outer coordination sphere (Hunter et al. 2007) The change in frequency separation $|\nu_1 - \nu_4|$ between symmetric and asymmetric stretching of the NO_3^- group can be used to differentiate between these biding states. The spectrum of complex 1 displays several intense bands at 1463 cm^{-1} (ν_1), 1031 cm^{-1} (ν_2), 815 cm^{-1} (ν_3) and 1284 cm^{-1} (ν_4) which may be assigned to the coordinated nitrate ion (C_{2v}), Fig. 1.

All complexes give a $|\nu_1 - \nu_4|$ separation in the range $177\text{--}180\text{ cm}^{-1}$ which suggests that all NO_3^- ions in the complexes coordinate to the metal ion as bi-dentate ligand (Yan et al. 2007). The band at $1384\text{--}1383\text{ cm}^{-1}$ in the spectra of the complexes indicates that a free nitrate group is present in

the outer sphere. The measured values of molar conductivities of all complexes strongly support the results obtained from the FT-IR data.

$^1\text{H-NMR}$ characterization

The $^1\text{H-NMR}$ spectra of the NHIso and complexes **1–8** were recorded in the range 0–15 ppm in deuterated dimethylsulphoxide, DMSO-d_6 solution. For the ligand, the proton of the hydroxyl group (OH) is assigned to the peak observed at 12.57 ppm. At 9.48 ppm and 8.84 ppm, two singlet peak are observed and assigned to the protons of the azomethine (CH=N) group, and of the NH group, respectively. The protons of the aromatic rings of the NHIso ligand are assigned in the range of $\delta = 7.25\text{--}7.98$ ppm. Complex **1** spectrum shows a slight shift in the singlet peak of the hydroxyl (OH) group with a value of 12.55 ppm. This shift is considered a slight high shift and group (Li et al. 2007). The peak due to azomethine proton appears at 9.44 ppm indicating the coordination of nitrogen atom azomethine (C=N) with the metal ion. The peak of NH group did not shift at all after complexation, which means that no coordination occurred between the La ion and NH group. All signals observed, in the spectrum, of the protons of the aromatic rings remained unchanged after complexation. This indicates that coordination occurred without deprotonation of the hydroxyl (OH).

$^{13}\text{C-NMR}$ characterization

$^{13}\text{C-NMR}$ spectra of the NHIso and its complexes were recorded in DMSO-d_6 . Two signals were observed at 164.97 and 143.74 ppm assigned to carbonyl (C=O) carbon and the azomethine carbon (C=N), in the spectrum of the free ligand, respectively. After complexation, the signal of C=O was shifted to 160.94 ppm, while the signal of C=N was shifted to 139.75 ppm. These shifts are a strong evidence of the coordination between these two groups with the La ion.

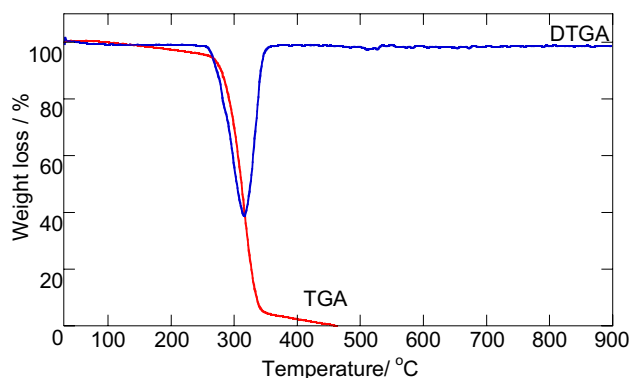


Fig. 2 TGA–DTGA thermo-grams for NHIso

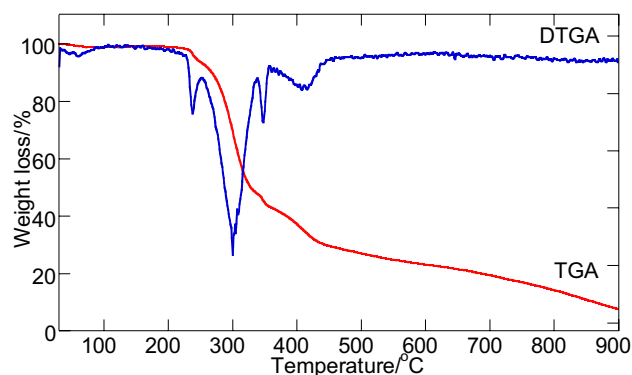


Fig. 3 TGA–DTGA thermo-grams for complex **1**

All Signal peaks present in the region $\delta = 114\text{--}136$ ppm are due to aromatic carbons.

Ultraviolet–visible (UV–vis) spectroscopy

UV–vis spectra of the NHIso ligand and complexes **1–8** were carried out at room temperature in DMSO. The wavelength (λ_{max}) values for all prepared substances are tabulated in Table 2. The absorption spectrum of the free NHIso ligand, shows four maxima at 326, 328, 347 and 416 nm. The bands observed at $\lambda_{\text{max}} = 326$ nm and $\lambda_{\text{max}} = 328$ nm are attributed to the $\pi - \pi^*$ transitions of the aromatic ring. A π

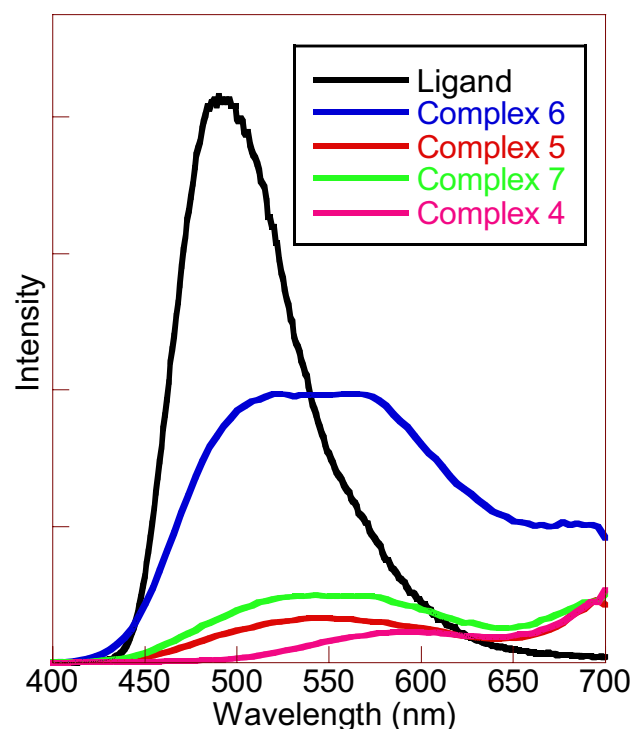


Fig. 4 Photoluminescence spectra of the ligand and complexes **4–7**

– π^* transition of the azomethine group $C=N$ may be attributed to the absorption band that exists at $\lambda_{\max} = 347$ nm. The presence of the lone pair of electrons of p-orbital of N-atom in $C=N$ will cause conjugation between them. This conjugation will cause a transition between $n - \pi^*$, appearing as a band with low energy at $\lambda_{\max} = 416$ nm.

The recorded spectra of complexes **1–8** are different from that of the ligand, suggesting coordination with metal ions. Two important changes were observed in the spectra due to complexation process between the ligand and the metal ions. In UV–vis region (300–650 nm) $\pi \rightarrow \pi^*$ n and $\rightarrow \pi^*$ absorption bands upon coordination, the two lower energy bands in **NHiso** are overlapped in a single band and shifted to shorter wavelength region (blue shift) (Keshavan et al. 2000). This shift is suggested to occur due to the electrons lone pair donation of the ligand's N-atom to the metal ions, which is consistent with that observed earlier (Keshavan et al. 2000). It was difficult to identify the absorption band due to the $f-f$ transition of the Ln(III) metal ions in the visible region of all complexes, because transitions of $f-f$ orbitals are very weak, and the strong charge transfer transition of the ligand will obscure the bands corresponding to these transitions (Raman et al. 2001).

Thermo-gravimetric analysis

Thermo-gravimetric (TG) and differential thermo-gravimetric (DTG) analysis were done under N_2 flow within the temperature range 25–900 °C. The ligand is considered thermally stable in the range 25–265 °C as shown from the TGA–DTG curve. The decomposition occurs in one step between 265 and 450 °C, Fig. 2, at maximum temperature of 315 °C, accompanied by a mass loss of 95.11%. The remaining weight may correspond to some ashes. All prepared complexes do not possess solvent molecules and/or water molecules according to their TGA–DTGA curves. These reported curves suggest that decomposition of the synthesized complexes, **1–8**, proceeds with four consecutive steps.

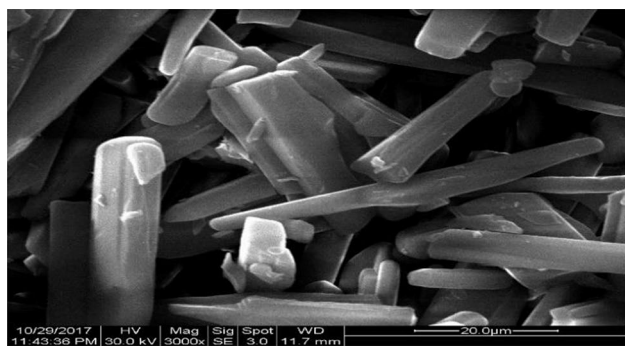


Fig. 5 SEM image of **NHiso**

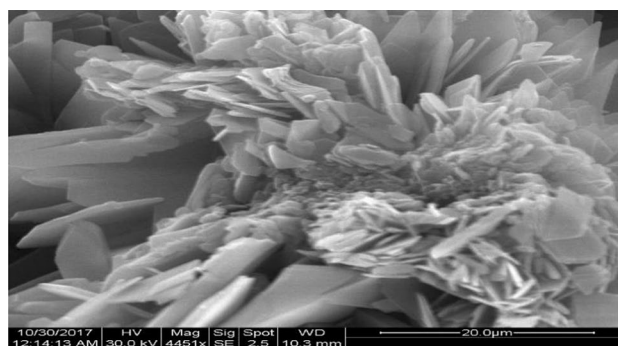


Fig. 6 SEM image of complex **2**

The thermal curves for complexes indicate that the compounds start losing mass with partial evaporation of organic ligand (1st step). The 2nd, 3rd and 4th steps involve the loss of one nitrate (NO_3) molecule from the outer sphere, two NO_3 molecules from the inner sphere and other part of the ligand, as shown in Fig. 3 for complex **1**.

Luminescence properties

The fluorescent properties of **NHiso** and complexes **4–7** were recorded in methanol at room temperature, Fig. 4. Pure **NHiso** demonstrates an intense emission band at 548 nm. This band could be assigned due to $\pi \rightarrow \pi^*$ transitions of the p electrons of the aromatic rings as well as $n \rightarrow \pi^*$ transitions of the $C=O$ and $C=N$ groups. The emission spectra of complexes **4–7** display only the ligand characteristic emission peaks with an obvious blue shift and a significant decrease in the fluorescence intensity. This indicating that **NHiso** is coordinated with lanthanide ions and cannot transfer the absorbed energy onto Ln(III) excited states.

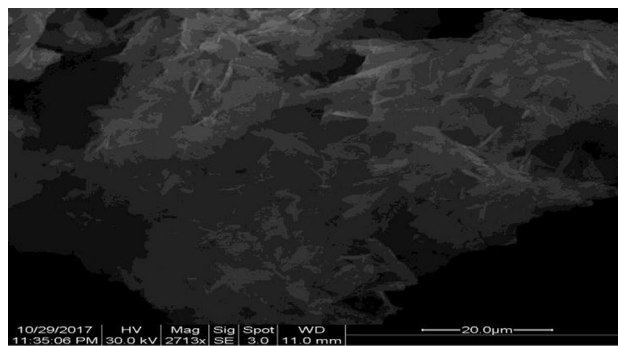


Fig. 7 SEM image of complex **7**

Table 3 MIC of NHIso and complexes **1–8** against a number of bacteria ($\mu\text{g/mL}$)

Tested compounds	Gram-negative bacteria				Gram-positive bacteria	
	<i>Ec</i>	<i>Kp</i>	<i>Pm</i>	<i>Pa</i>	<i>Sa</i>	<i>En</i>
NHIso	N	N	N	N	16	32
Complex 1	N	N	N	N	8	16
Complex 2	N	N	N	N	4	4
Complex 3	N	N	N	N	16	32
Complex 4	N	N	N	N	8	16
Complex 5	N	N	N	N	16	32
Complex 6	N	N	N	N	16	32
Complex 7	N	N	N	N	8	16
Complex 8	N	N	N	N	16	16
DMSO (–ve control)	N	N	N	N	N	N
Oxytetracycline(+ve control)	2	4	8	2	8	8

Ec *Escherichia coli*; *Kp* *Klebsiella pneumoniae*; *Pm* *Proteus mirabilis*; *Pa* *Pseudomonas aeruginosa*; *En* *Enterococcus faecalis*; *Sa* *Staphylococcus aureus*

N None active compound

Scanning electron micrographs (SEM)

SEM for **NHIso**, complex **2** and complex **7** are shown in Figs. 5, 6 and 7, respectively. **NHIso** image shows that it exists as almost cylindrical rods. Clear and obvious changes in the structures morphology of complexes **2** and **7** exist compared to **NHIso**, which indicates the formation of complexes. The SEM images of both complexes are almost the same.

Antimicrobial activity

The bactericidal screening results of **NHIso** and the synthesized complexes are recorded in Table 3. MIC was defined as the minimal concentration that has optical density less than that of the Oxytetracycline which is the positive control. **NHIso** ligand and its complexes showed various degree of MIC on the growth of the bacterial strain tested. Results indicated that the ligand showed a significant antibacterial activity against *Enterococcus faecalis* (*En*) and *Staphylococcus*

aureus (*Sa*). No activity toward any of the Gram-negative bacteria have been recorded. Comparing these results with the *N*-(2-hydroxynaphthalen-1-yl) methylene) nicotinohydrazide Schiff base (Hijazi et al. 2017a), it is clear that the reported isonicotinohydrazide ligand (**NHIso**) is selective toward Gram-positive bacteria with better MIC values (16 and 32 $\mu\text{g/mL}$ than that for nicotinohydrazide (MIC values for *Sa* and *En* are 64 and 256 $\mu\text{g/mL}$, respectively). Many groups may play an important role in the activity against different strains of bacteria, two groups present in the investigated **NHIso** ligand are the hydroxyl and azomethine, their presence is the cause of the promising activity of the ligand against Gram-positive bacteria (Azza et al. 2009). All synthesized complexes were selective toward Gram-positive bacteria only and possessed excellent antibacterial activities against *Staphylococcus aureus* and *Enterococcus faecalis*, especially complex **2**, which showed the highest value of 4 $\mu\text{g/mL}$. All complexes showed no activity toward the tested Gram-negative bacteria. Complexes **1**, **2**, **4**, **7** and **8** showed higher activities against Gram-positive bacteria than

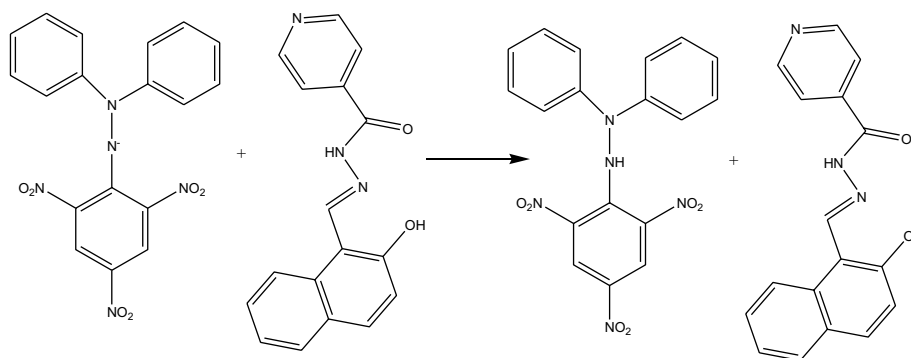
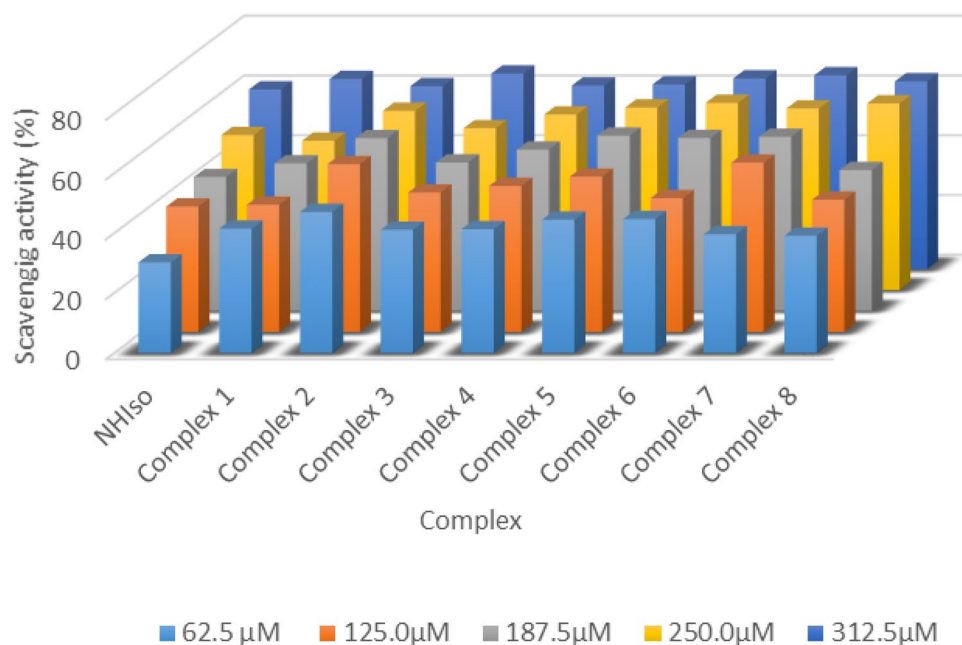
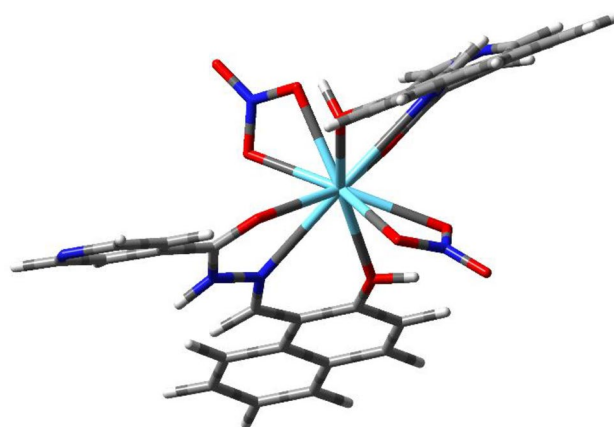
Scheme 2 Scavenging activity proposed mechanism for **NHIso**

Fig. 8 DPPH scavenging activity of NHIso and complexes 1–8**Table 4** Antioxidant scavenging activity results of NHIso and complexes 1–8

Complex	DPPH scavenging activity (%)				
	62.50	125.0	187.5	250.0	312.5
NHIso	30.2 ± 0.2	41.9 ± 0.9	44.8 ± 0.4	51.9 ± 0.2	60.2 ± 0.4
Complex 1	41.5 ± 0.3	42.5 ± 0.6	49.4 ± 0.5	50.0 ± 0.2	63.7 ± 0.4
Complex 2	47.1 ± 0.9	56.1 ± 0.6	57.8 ± 0.8	60.0 ± 0.2	61.3 ± 1.3
Complex 3	41.1 ± 1.3	46.6 ± 1.0	49.7 ± 1.5	54.2 ± 1.1	65.5 ± 0.5
Complex 4	41.3 ± 1.1	48.8 ± 1.1	54.0 ± 0.3	58.8 ± 1.4	61.5 ± 1.0
Complex 5	44.5 ± 1.5	51.9 ± 0.2	58.7 ± 0.7	61.1 ± 0.3	61.9 ± 0.1
Complex 6	44.7 ± 0.5	44.7 ± 0.3	57.9 ± 0.1	62.7 ± 0.7	63.9 ± 1.2
Complex 7	39.6 ± 0.1	56.6 ± 0.6	58.3 ± 1.5	60.8 ± 0.7	64.9 ± 0.1
Complex 8	39.1 ± 0.9	44.2 ± 0.2	47.2 ± 0.5	62.5 ± 0.4	62.9 ± 0.6

the NHIso free ligand. Their previously reported nicotino-hydrazide complexes (Hijazi et al. 2017a) showed different and variable activities toward Gram-negative and Gram-positive bacteria. It is obvious that the currently reported complexes, 1–8, have showed selective and much better activities against Gram-positive bacteria, *Sa* & *En*, ranging from 4 to 32 μg/mL, than that of their nicotinohydrazide analogues with a MIC values between 16 and 256 μg/mL. The activity enhancement is due to the reduction of the polarity of the lanthanide ions. This reduction may arise from the partial sharing of the positive charge on the Ln ions with the N and O donor atoms and may be because of the electron delocalization over the entire system (Abdel-Rahman et al. 2016a, b; Abdel-Rahman et al. 2020). The central atom lipophilic nature will increase, which increases the complexes penetration into the lipid membrane of the microorganism cell wall. This penetration process may raise the complex activity, restricting further growth of the organism. In Gram-negative

**Fig. 9** Optimized ground state geometry of $[La(NHIso)_2(NO_3)_2]^+$

bacteria, and on their surfaces, Lipopoly Saccharide (LPS) is found to be one of the major components, in addition to peptidoglycan layer. Lipopolysaccharide is critical in maintaining the barrier function preventing the passive diffusion of hydrophobic solutes. In contrast, Gram-positive bacteria, lack an outer lipid membrane, but contain a cytoplasmic membrane bordered by a layer of peptidoglycan.

Antioxidant activity

Determination of the NHiso ligand and complexes **1–8** as free radical scavengers, is performed using DPPH. The DPPH test is based on the ability of the stable 2, 2-diphenyl-1-picrylhydrazyl free radical to react with hydrogen donors (Inoue et al. 2005; Fahey and Stephenson; 2002). As stable nitrogen-centered free radical, DPPH is characterized by the delocalization of spare electron over the molecule, giving a strong absorption maximum at 517 nm in purple color. By mixing a free radical scavenging antioxidant substance with the used free radical, which can donate a hydrogen atom, DPPH-H will form from the pairing of the odd electron of the radical with hydrogen from the substance investigated as an antioxidant. This process is accompanied by a change in color from purple to yellow, scheme 2. Figure 8 shows the plots of DPPH scavenging activity percent for NHiso and complexes **1–8**. The scavenging activity was calculated using the following equation:

$$\% \text{ Scavenging Activity} = \frac{(A_0 - A_s) \times 100\%}{A_0},$$

where A_0 is the absorbance of the DPPH in the absence of the tested samples and after shaking (control) and A_s is the absorbance of the DPPH in the presence of tested compound.

The antioxidant activity of all tested complexes was found to be concentration dependent and as the concentrations of the tested compounds increase, the scavenging ratio increases in required range, Table 4. The NHiso free ligand was found to have an activity between 30 and 60% within investigated concentration range due to the key role of the functional group, OH, by forming stable macromolecular radicals when reacting with used radical by the H-abstraction. It is clear that complexes **1–8** have more efficiency in quenching DPPH than that of characterized by virtue of delocalization of spare electron their free NHiso ligand, with activities between 39 and 65%, Table 4 and Fig. 8. These activities are higher than the reported ones for the nicotinothiazide complexes, ranging from 13 to 60%. The efficiency of NHiso ligand in quenching DPPH is much better than it's *N*-(2-hydroxynaphthalen-1-yl) methylene) nicotinothiazide Schiff base analogue (Hijazi et al. 2017a). NHiso showed activities between

30 and 60%, while the nicotinothiazide showed activities between 13 and 22% only. These numbers could be attributed to the fact that DPPH radical scavenging assay is an electron transfer (ET)-based method with mechanism of Hydrogen Atom Transfer (HAT) (Cao et al. 1996; Prior et al. 2005).

DFT calculations

The optimized ground state structure of $[\text{La}(\text{NHiso})_2(\text{NO}_3)_2]^+$ cation at B3LYP level of theory (Fig. 9) are in a good agreement with the expected experimental data. It shows that Lanthanum has 10 coordination number. The two nitrate ligand has 4 coordination. Each nitrate acts as bi-dentate ligand through two oxygen atoms with La–O bond distance 2.56 Å and 2.60 Å. The other 6 coordination came from the two Schiff base ligands in which the bond length in La–O=C, La–OH–C and La–N=N are 2.54 Å, 2.68 Å and 2.89 Å, respectively, for one of the Schiff base ligand. For the other one, the bond lengths are 2.54 Å, 2.65 Å, and 2.87 Å. The vibration frequency of C=N is 1620 cm^{-1} and 1615 cm^{-1} for the first and second ligand. The vibrational frequency of the two C=O are 1637 cm^{-1} and 1639 cm^{-1} . The decreasing of the vibration frequency of the C=N and C=O as result of the coordination agrees with the experiments and support the proposed structure of the complex.

Conclusion

In this work, *N*-(2-hydroxynaphthalen-1-yl) methylene) Isonicotinothiazide, **NHiso**, Schiff base ligand and its synthesized lanthanide complexes **1–8** characterized using different techniques. The ligand was concluded to be a bi-dentate chelate being coordinated to the central lanthanide ion in a 2:1 stoichiometric ratio by the two azomethine nitrogen atoms and the two carbonyl oxygen atoms. The molar conductance values showed that one nitrate group is coordinated through the outer coordination sphere for all complexes. IR spectral data also reveal that the two nitrate NO_3^- groups coordinated to lanthanide metal ions bi-dentately in all complexes. So, coordination number ten is suggested for metal ion in all prepared complexes. The antimicrobial activities of complexes **1–8** were studied against different strains of bacteria, (Gram-negative bacteria) and (Gram-positive bacteria). Complexes **1, 2, 4, 7** and **8** showed significant and higher activity against *En: Enterococcus faecalis* and *Sa: Staphylococcus aureus* Gram-positive bacteria than the NHiso ligand, especially complex **2** with a MIC value of 4 $\mu\text{g}/\text{mL}$. The antioxidant activities of all prepared complexes are concentration

dependent and the scavenging values increase with the increase in sample concentration in the tested range showing much more efficiency in quenching DPPH than the NHIso ligand, with a scavenging activity between 39 and 65%. Future work must focus on the synthesis of new Schiff bases containing different functional groups, which may improve the activities of the compounds. The antimicrobial studies should be conducted *in vivo*, as well as the study of antimalarial, antifungal, anti-inflammatory and antiviral properties of the synthesized complexes.

Authors contribution AKH involved in conceptualization, investigation, methodology, project administration, resources, roles/writing—original draft and writing—review and editing. ZAT participated in data curation, formal analysis and writing—review and editing. IMI involved in investigation and formal analysis. AI participated in software, data curation and formal analysis. WMAI-M involved in investigation and methodology.

Funding Deanship of Scientific Research, Jordan University of Science and Technology is acknowledged for financial support (project no. 110/2017).

Data availability The datasets generated during and/or analyzed during the current study are available from the corresponding author.

Declarations

Conflict of interest The authors declare no conflict of interest.

References

- Abdel-Rahman LH, Abu-Dief AM, Basha M, Abdel-Mawgoud AAH (2017a) Three novel Ni(II), VO(II) and Cr(III) mononuclear complexes encompassing potentially tridentate imine ligand: synthesis, structural characterization, DNA interaction, antimicrobial evaluation and anticancer activity. *Appl Organomet Chem*. <https://doi.org/10.1002/aoc.3750>
- Abdel-Rahman LH, Abu-Dief AM, Adam MSS, Hamdan SK (2016a) Some new nano-sized mononuclear Cu(II) Schiff base complexes: design, characterization, molecular modeling and catalytic potentials in benzyl alcohol oxidation. *Catal Lett* 146:1373–1396. <https://doi.org/10.1007/s10562-016-1755-0>
- Abdel-Rahman LH, Abu-Dief AM, Moustafa H, Hamdan SK (2017b) Ni(II) and Cu(II) Complexes with ONNO asymmetric tetradentate schiff base ligand: synthesis, spectroscopic characterization, theoretical calculations, DNA interaction and antimicrobial studies. *Appl Organomet Chem*. <https://doi.org/10.1002/aoc.3555>
- Abdel-Rahman LH, Abu-Dief AM, Ismael M, Mohamed MAA, Hashem NA (2016b) Synthesis, structure elucidation, biological screening, molecular modelling and DNA binding of some Cu(II) chelates incorporating imines derived from amino acids. *J Mol Struct* 1103:232–244. <https://doi.org/10.1016/j.molstruc.2015.09.039>
- Abdel-Rahman LH, Adam MS, Abu-Dief AM, El-Sayed Ahmed H, Nafady A (2020) Non-linear optical property and biological assays of therapeutic potentials under *in vitro* conditions of Pd(II), Ag(I) and Cu(II) complexes of 5-diethyl amino-2-((2-[(2-hydroxybenzylidene)-amino]-phenylimino)-methyl)-phenol. *Molecules*. <https://doi.org/10.3390/molecules25215089>
- Abu-Dief AM, Abdel-Rahman LH, Abdel-Mawgoud AAH (2020) A robust *in vitro* anticancer, antioxidant and antimicrobial agents based on new metal-azomethine chelates incorporating Ag(I), Pd (II) and VO (II) cations: probing the aspects of DNA interaction. *Appl Organomet Chem*. <https://doi.org/10.1002/aoc.5373>
- Agarwala BV, Hingorani S, Nagana Gowda GA (1990) Synthetic and physicochemical studies of uranium complexes with semicarbazone and hydrazine. *Inorg Chim Acta* 176:149–154. [https://doi.org/10.1016/S0020-1693\(00\)85106-3](https://doi.org/10.1016/S0020-1693(00)85106-3)
- Ajlouni AM, Taha ZA, Hijazi AK, Al Momani WM (2018) A Series of lanthanide complexes with 2-fluoro-*N'*-(furan-2-ylmethylene) benzohydrazide ligand: synthesis, characterization, luminescent properties and biological evaluation. *Appl Organomet Chem*. <https://doi.org/10.1002/aoc.4536>
- Ajlouni AM, Hijazi AK, Taha ZA, Al Momani W, Okour A, Kühn FE (2019) Synthesis, characterization and biological and catalytic activities of propionitril: ligated transition metal complexes with [B(C₆F₅)₄] as counter anion. *Cat Lett* 149:2317–2324. <https://doi.org/10.1007/s10562-019-02804-9>
- Al Momani W, Taha ZA, Ajlouni AM, Shaqra Q, Zoubi M (2013) A study of *in vitro* antibacterial activity of lanthanides complexes with a tetradentate schiff base ligand. *Asian J Trop Biomed* 3:367–370. [https://doi.org/10.1016/S2221-1691\(13\)60078-7](https://doi.org/10.1016/S2221-1691(13)60078-7)
- Ameen I, Tripathi AK, Mishra RL, Siddiqui A, Tripathi UN (2018) A study on enhancing the quantum yield and antimicrobial activity of Pr(III) by varying the coordination environment. *RSC Adv* 8:8412–8425. <https://doi.org/10.1039/c7ra13035j>
- Andres J, Chauvin AS (2020) Colorimetry of luminescent lanthanide complexes. *Molecules*. <https://doi.org/10.3390/molecules25174022>
- Avaji PG, Kumar CHV, Patil SA, Shivananda KN, Nagaraju C (2009) Synthesis, spectral characterization, *in vitro* microbiological evaluation and cytotoxic activities of novel macrocyclic bis hydrazine. *Eur J Med Chem* 44:3552–3559. <https://doi.org/10.1016/j.ejmech.2009.03.032>
- Aziz AN, Taha M, Ismail NH, Anouar EH, Yousuf S, Jamil W, Awang K, Ahmat N, Khan KM, Kashif SM (2014) Synthesis, crystal structure, DFT studies and evaluation of the antioxidant activity of 3,4-dimethoxybenzenamine Schiff bases. *Molecules* 19:8414–8433. <https://doi.org/10.3390/molecules19068414>
- Azza A, Abou-Hussen A, Linert W (2009) Chromotropism behavior and biological activity of some schiff base-mixed ligand transition metal complexes. *Syn React Inorg Metaorg Nanometal Chem* 39:570–599. <https://doi.org/10.1080/15533170903327950>
- Bayrak H, Demirbas N, Karaoglu SA (2009) Synthesis of some new 1,2,4-triazoles starting from isonicotinic acid hydrazide and evaluation of their antimicrobial activities. *Eur J Med Chem* 44:4362–4366. <https://doi.org/10.1016/j.ejmech.2009.05.022>
- Biradar NS, Kulkarni VH (1971) A spectroscopic study of Tin(IV) complexes with bidentate Schiff bases. *J Inorg Nucl Chem* 33:2451–2457. [https://doi.org/10.1016/0022-1902\(71\)80220-8](https://doi.org/10.1016/0022-1902(71)80220-8)
- Belicchi FM, Bisceglie F, Pelosi G (2001) Synthesis, characterization, x-ray structure and biological activity of three new 5-formyluracil thiosemicarbazone complexes. *J Inorg Biochem* 83:169–179. [https://doi.org/10.1016/S0162-0134\(00\)00181-1](https://doi.org/10.1016/S0162-0134(00)00181-1)
- Bünzli JCG (2008) Review: lanthanide coordination chemistry: from old concepts to coordination polymers. *J Coord Chem* 67:3706–3733. <https://doi.org/10.1080/00958972.2014.957201>
- Cai LL, Zhang SM, Li Y, Wang K, Li XM, Müller G, Liang FP, Hu YT, Wang GX (2021) Lanthanide nitrate complexes bridged by the bis-tridentate Ligand 2,3,5,6-tetra(2-pyridyl)pyrazine: synthesis, crystal structures, hirshfeld surface analyses, luminescence

- properties, DFT calculations, and magnetic behavior. *J Luminescence*. <https://doi.org/10.1016/j.jlumin.2020.117835>
- Canpolat E, Kaya M (2004) Studies on mononuclear chelates derived from substituted Schiff-base ligands (part 2): synthesis and characterization of a new 5-bromosalicyliden-p-aminoacetophenone-oxime and its complexes with Co(II), Ni(II), Cu(II) and Zn(II). *J Coord Chem* 57:1217–1223. <https://doi.org/10.1080/00958970412331285913>
- Cao G, Sofic E, Prior R (1996) Antioxidant capacity of tea and common vegetables. *J Agric Food Chem* 44:3426–3431. <https://doi.org/10.1021/jf9602535>
- Chandrasekhar V, Das S, Dey A, Hossain S, Sutter JP (2013) Tetranuclear lanthanide (III) complexes containing dimeric subunits: single-molecule magnet behavior for the Dy₄ analogue. *Inorg Chem* 52:11956–11965. <https://doi.org/10.1021/ic401652f>
- Desoky A, Mohamad M, Abualreish MJA, Abu-Dief AM (2019) Antimicrobial and anticancer activities of cobalt (III)-hydrazone complexes: solubilities and chemical potentials of transfer in different organic co-solvent-water mixtures. *J Molec Liq*. <https://doi.org/10.1016/j.molliq.2019.111162>
- Donia AM, El-Boraey HA (2002) Preparation of highly insulating dimeric and polymeric metal complexes with higher thermal stability in the solid state. *J Anal Appl Pyrolysis* 63:69–84. [https://doi.org/10.1016/S0165-2370\(01\)00142-5](https://doi.org/10.1016/S0165-2370(01)00142-5)
- Fahey JW, Stephenson KK (2002) Pinostrobin from Honey and Thai Ginger (*Boesenbergia pandurata*): a potent flavonoid inducer of mammalian phase 2 chemoprotective and antioxidant enzymes. *J Agric Food Chem* 50:7472–7476. <https://doi.org/10.1021/jf025692k>
- Gao B, Zhang L, Zhang D (2018) Synthesis and characterization of two novel schiff base type macromolecular ligands and preliminary research on luminescent property of polymer- rare earth complexes. *J Polym Res*. <https://doi.org/10.1007/s10965-017-1436-8>
- Geary W (1971) The use of conductivity measurements in organic solvents for the characterisation of coordination compounds. *Coord Chem Rev* 7:81–122. [https://doi.org/10.1016/S0010-8545\(00\)80009-0](https://doi.org/10.1016/S0010-8545(00)80009-0)
- Ghozlan SAS, Al-Omar MA, Amr AEE, Ali KA, Abd El-Wahab AA (2011) Synthesis and antimicrobial activity of some heterocyclic 2,6-bis(substituted)-1,3,4-thiadiazolo-, oxadiazolo-, and oxathiazolidino-pyridine derivatives from 2,6-pyridine dicarboxylic acid dihydrazide. *J Hetero Chem* 48:1103–1110. <https://doi.org/10.1002/jhet.690>
- Gudasi KB, Havanur VC, Patil SA, Patil BR (2007) Antimicrobial study of newly synthesized lanthanide(III) complexes of 2-[2-hydroxy-3-methoxyphenyl]-3-[2-hydroxy-3-methoxybenzylamino]-1,2-dihydroquinazolin-4(3H)-one. *Met Based Drugs*. <https://doi.org/10.1155/2007/37348>
- Gulerman NN, Oruc EE, Kartal F, Rollas S (2000) In Vivo metabolism of 4-fluorobenzoic acid [(5-nitro-2-furanyl) methylene] Hydrazide in Rats. *Eur J Drug Metab Pharmacokin* 25:103–108. <https://doi.org/10.1007/BF03190075>
- Hijazi AK, Taha ZA, Ajlouni AM, Al-Momani WM, Idris IM, Hamra EA (2017a) Synthesis and biological activities of lanthanide (III) nitrate complexes with N-(2-hydroxynaphthalen-1-yl) methylene) Nicotinohydrazide Schiff base. *Med Chem* 13:77–84. <https://doi.org/10.2174/1573406412666160225155908>
- Hijazi AK, Taha ZA, Ajlouni AM, Al Momani WM, Ababneh TS, Alshare HM, Kühn FE (2017b) Synthesis, catalytic and biological activities and computational study of Fe(III) solvent-ligated complexes having B(Ph)₄ as counter anion. *Appl Organomet Chem*. <https://doi.org/10.1002/aoc.3601>
- Hijazi AK, Taha ZA, Ababneh TS, Alshare HM, Al-Bataineh N, Al Momani WM, Ajlouni AM (2020) In vitro biological, catalytic, and DFT studies of some iron(III) N-ligated complexes. *Chem Pap* 74:1561–1572. <https://doi.org/10.1007/s11696-019-01009-z>
- Hijazi AK, Taha ZA, Al-Dawood LA, Ababneh TS, Al-Momani WM (2021) Catalytic cyclopropanation, antimicrobial, and DFT properties of some chelated transition metal(II) complexes. *J Mol Struct*. <https://doi.org/10.1016/j.molstruc.2020.129733>
- Hunter AP, Lees AMJ, Platt AWG (2007) Synthesis, structures and mass spectrometry of lanthanide nitrate complexes with tricyclohexylphosphine oxide. *Polyhedron* 26:4865–4876. <https://doi.org/10.1016/j.poly.2007.06.023>
- Inoue K, Murayama S, Seshimo F, Takeba K, Yoshimura Y, Nakazawa H (2005) Identification of phenolic compound in manuka honey as specific superoxide anion radical scavenger using electron spin resonance (ESR) and liquid chromatography with coulometric array detection. *J Sci Food Agric* 85:872–878. <https://doi.org/10.1002/jsfa.1952>
- Jin CW, Zhao QQ, Ren N, Zhang JJ, Geng LN, Wang SP, Shi SK (2017) Preparation, crystal structures and properties of a series of novel lanthanide complexes based on 2,3-dimethoxybenzoic acid and 1,10-phenanthroline. *Polyhedron* 135:206–215. <https://doi.org/10.1016/j.poly.2017.06.050>
- Keshavan B, Chandrashekar PG, Made-Gowda NM (2000) Synthesis, characterization, and spectral studies of lanthanide(iii) nitrate complexes of promethazine. *J Mol Struct* 553:193–197. [https://doi.org/10.1016/S0022-2860\(00\)00551-2](https://doi.org/10.1016/S0022-2860(00)00551-2)
- Khan AA, Sharma NK (2008) Synthesis and physico-chemical investigations of some seven coordinated complexes of lanthanides(iii) chloride derived from hydrazones of isonicotinic acid hydrazide. *Asian J Chem* 20:4969–4979. <https://doi.org/10.14233/ajchem.2008.6489>
- Kumar D, Sundaree S, Johnson EO, Shah K (2009) An efficient synthesis and biological study of novel indolyl-1,3,4-oxadiazoles as potent anticancer agents. *Bioorg Med Chem Lett* 19:4492–4494. <https://doi.org/10.1016/j.bmcl.2009.03.172>
- Kuriakose M, Kurup MRP, Suresh E (2007) Spectral characterization and crystal structure of 2-benzoylpyridine nicotinoyl hydrazine. *Spec Chim Acta Sec A* 66:353–358. <https://doi.org/10.1016/j.saa.2006.03.003>
- Li T, Yang Z, Wang BD (2007) Synthesis, characterization and anti-oxidative activity of new rare earth complexes of 6-hydroxy chromone-3-carbaldehyde-(4'-hydroxy)benzoyl hydrazine. *J Coord Chem* 60:597–605. <https://doi.org/10.1080/0095897060895896>
- Mohanank, Kumari BS, Rijulal G (2008) Microwave assisted synthesis, spectroscopic, thermal and antifungal studies of some lanthanide(iii) complexes with a heterocyclic bishydrazone. *J Rare Earths* 26:16–21. [https://doi.org/10.1016/S1002-0721\(08\)60028-9](https://doi.org/10.1016/S1002-0721(08)60028-9)
- Palai YN, Anjali K, Sakthivel A, Ahmed M, Sharma D, Badamali SK (2018) Cerium ions grafted on functionalized mesoporous SBA-15 molecular sieves: preparation and its catalytic activity on p-cresol oxidation. *Cat Lett* 148:465–473. <https://doi.org/10.1007/s10562-017-2238-7>
- Pandey UK, Pandey OP, Sengupta SK, Tripathi SC (1987) Syntheses and spectroscopic studies on tetraaza macrocyclic complexes of praseodymium(III). *Polyhedron* 6:1611–1617. [https://doi.org/10.1016/S0277-5387\(00\)80848-7](https://doi.org/10.1016/S0277-5387(00)80848-7)
- Prior RL, Wu X, Schaich K (2005) Standardized methods for the determination of antioxidant capacity and phenolics in foods and dietary supplements. *J Agric Food Chem* 53:4290–4302. <https://doi.org/10.1021/jf0502698>
- Raman N, Kulan-Sdaisamy A, Shunmugasundaram A, Jeyasubramanian K (2001) Synthesis, spectral, redox and antimicrobial activities of schiff base complexes derived from 1-phenyl-2,3-dimethyl-4-aminopyrazol-5-one and acetoacetanilide. *Trans Metal Chem* 26:131–135. <https://doi.org/10.1023/A:1007100815918>

- Sengupta SK, Pandey OP, Srivastava BK, Sharma VK (1998) Synthesis, structural and biochemical aspects of titanocene and zirconocene chelates of acetylferrocenyl thiosemicarbazones. *Trans Metal Chem* 23:349–435. <https://doi.org/10.1023/A:10069861314353>
- Singh K, Barwa M, Tyagi P (2007) Synthesis and characterization of cobalt(II), nickel(II), copper(II) and zinc(II) complexes with schiff base derived from 4-amino-3-mercapto-6-methyl-5-oxo-1,2,4-triazine. *J Med Chem* 42:394–402. <https://doi.org/10.1016/j.ejmech.2006.10.016>
- Taha ZA, Hijazi AK (2021) Structural and Photophysical properties of lanthanide complexes with N'-(2-methoxybenzylidene)-2-pyridinecarbohydrazide Schiff base ligand: catalyzed Oxidation of Anilines with Hydrogen Peroxide. *J Mol Struct.* <https://doi.org/10.1016/j.molstruc.2021.130451>
- Taha M, Ismail NH, Baharudin MS, Lalani S, Mehboob S, Khan KM, Yousuf S, Siddiqui S, Rahim F, Choudhary MI (2015) Synthesis crystal structure of 2-methoxybenzoylhydrazones and evaluation of their α -glucosidase and urease inhibition potential. *Med Chem Res* 24:1310–1324. <https://doi.org/10.1007/s00044-014-1213-8>
- Taha ZA, Ababneh TS, Hijazi AK, Abu-Salem Q, Ajlouni AM, Ebwany S (2018) Synthesis, density functional theory calculations and luminescence of lanthanide complexes with 2,6-bis[(3-methoxybenzylidene)hydrazinocarbonyl] pyridine Schiff base ligand. *Luminescence* 33:79–88. <https://doi.org/10.1002/bio.3375>
- Taha ZA, Ajlouni AM, Ababneh TS, Al Momani WM, Hijazi AK, Al Masri M, Hammad H (2017a) DFT computational studies, biological and antioxidant activities, and kinetic of thermal decomposition of 1, 10-phenanthroline lanthanide complexes. *Struct Chem* 28:1907–1918. <https://doi.org/10.1007/s11224-017-0975-2>
- Taha ZA, Hijazi AK, Ababneh TS, Mhaidat I, Ajlouni AM, Al-Hassan KA, Mitzithra C, Hamilakis S, Danladi F, Altalafha AY (2017b) Photophysical properties and computational study of newly synthesized lanthanide complexes with N-(2-carboxyphenyl) salicylideneimine Schiff base ligand. *J Luminescence* 181:230–239. <https://doi.org/10.1016/j.jlumin.2016.09.019>
- Taha ZA, Hijazi AK, Al Momani WM (2020) Lanthanide complexes of the tridentate Schiff base ligand salicylaldehyde-2-picolinoyl-hydrazone: synthesis, characterization, photophysical properties, biological activities and catalytic oxidation of aniline. *J Mol Struct.* <https://doi.org/10.1016/j.molstruc.2020.128712>
- Wang J, Wang H, Ma Y, Tang J, Li L, Wang Q, Zhao B, Cheng P, Ma J (2019) Enhancing magnetic behaviors of dysprosium single-molecule magnets from crystal field perturbation by deprotonating Schiff-Base ligand. *Cryst Growth Des* 19:3365–3371. <https://doi.org/10.1021/acs.cgd.9b00261>
- Xu DF, Xu YM, Chen NN, Zhou XA, Shi Y, He QZ (2010) Synthesis, characterization, and biological studies of lanthanide complexes with 2,6-pyridine dicarboxylic acid and α -picolinic acid. *J Coord Chem* 63:2360–2369. <https://doi.org/10.1080/00958972.2010.499937>
- Yan P, Sun W, Li G, Nei C, Gao T, Yu Z (2007) Synthesis, characterization and fluorescence of lanthanide schiff-base complexes. *J Coord Chem* 60:1973–1982. <https://doi.org/10.1080/009589707.1217602>

Publisher's Note Springer Nature remains neutral with regard to jurisdictional claims in published maps and institutional affiliations.

Authors and Affiliations

Ahmed K. Hijazi¹ · Ziyad A. Taha¹ · Abdellatif Ibdah¹ · Idris M. Idris¹ · Waleed M. Al-Momani²

✉ Ahmed K. Hijazi
akhijazi@just.edu.jo

² Department of Basic Medical Sciences, Faculty of Medicine, Yarmouk University, Irbid, Jordan

¹ Department of Chemical Sciences, Faculty of Science and Arts, Jordan University of Science and Technology, P.O. Box 3030, Irbid 22110, Jordan